IJIREEICE

ISSN (Online) 2321-2004
ISSN (Print) 2321- 5526

International Journal of Innovative Research in Electrical, Electronics, Instrumentation and Control Engineering

NFTPCOS-18

National Conference on Future Technologies in Power Control and Communication Systems

College of Engineering Perumon, Kollam, Kerala

Vol. 1, Special Issue 2, March 2018

Solar Powered Dual Inverter Fed Induction Motor with Open End Windings and its Control Algorithms for Pumping Applications

Rıya Anna Thomas[1], Reema N[2], Dhanusha T[3]

PG Scholar[1], Assistant Professor[2], PG Scholar[3] Dept. of Electrical and Electronics Engineering
Sree Buddha College of Engineering, Pattoor, India

Abstract: Induction motors are the widely used machines in many industrial applications. But the induction motors results in high starting current, occurrence of common mode voltages, difficult to control etc. This work proposes controlling of a dual inverter fed induction motor with open end stator windings. The three level dual inverter received large attention due to its simplicity and it reduces the voltage rating of the semiconductor devices which further reduces cost of the system. This system is operated using an integrated control which includes maximum power point tracking and space vector pulse width modulation technique. A boosting converter with a high voltage gain is also used which requires no chemical storage elements such as batteries and make the system more effective. For tracking the maximum power Perturb and observe method is used. Space vector modulation is designed such that it eliminates the common mode voltages generated and has less distortions compared to the conventional methods. The modeling of dual inverter fed open end winding induction motor, conventional induction machine, PV system, MPPT algorithm, Dickson charge pump and switching of inverters using space vector modulation has been done and the output waveforms obtained are analyzed.

Keywords: Common mode voltage, Dickson charge pump, Open end winding induction motor, Space vector modulation.

I. INTRODUCTION

Nowadays several countries across the world suffer from scarcity of water especially in rural areas. In such places, where shortage of electric power is a concern rules out the pumping and water treatments. One of the efficient solution is the use of systems supplied by photovoltaic solar energy. For consumer and industrial applications several high speed machines are gaining attention and this machine is a solution for pumping in rural areas. Among different machines, induction machines are most widely used due to many advantages such as low cost, ease of operation, durability, high starting torque, high efficiency etc. But the induction motors has certain disadvantages such as difficult to control, occurrence of common mode voltages, high starting current etc. Several multilevel converter topologies have also been analysed and proposed during several decades [1]-[3]. Some of the commonly used converter topologies include diode clamped, flying capacitor, and cascaded converters in order to obtain multilevel output waveforms. Less amount of voltage will be transferred by the diode which reduces the stress on other electrical devices and it provide multiple voltage output levels. This topology produces the output voltage which is only half the direct current voltage and capacitor balancing is also a major issue. To improve the overall performance neutral point clamped inverters was used which is advantageous over two level H bridge inverter [4]. Neutral point clamped have advantages such as high power quality, low electromagnetic interference etc but these inverters requires more clamping diodes and produces neutral point fluctuations. The multilevel inverter is a viable solution for the voltage limits of power switching converters and are able to generate output voltage waveforms with large number of steps from the voltage sources of lower level. Multilevel inverters have several advantages such as improved voltage waveform, less harmonic distortion, high switching frequency etc and is suitable for medium voltage, high power motor drives and low voltage, high efficiency systems. Among these inverters dual inverters are widely used due to its simplicity and fault tolerant capacity. Furthermore if one of the inverter is failed, the outputs can be short circuited and the system can be operated as single sided three phase inverter. Nowadays for high speed applications multiphase winding machines are commonly adopted for different applications in hybrid and electric vehicles etc. In this paper, a three level dual inverter fed open end winding induction motor is proposed to overcome the disadvantages of conventional induction motor. Vast works were carried out for different inverter topologies [5]-[8] and different modulation schemes [9]-[10] for open end winding induction motor. In this machine stator windings are open and the supply is given from both sides and inverters are connected at either ends to obtain the multilevel output. The system is supplied by solar panel and MPPT algorithm is also used to track the maximum power and space vector modulation scheme is also used for switching of inverters.

II. CONTROL ALGORITHMS OF OEWIM

The proposed system includes control algorithms for an open end winding induction motor (OEWIM) and modified Dickson charge pump. OEWIM is simply an induction motor with both the ends of the stator windings are opened [11]-[13].The figure 1 shows the block diagram of the proposed system.

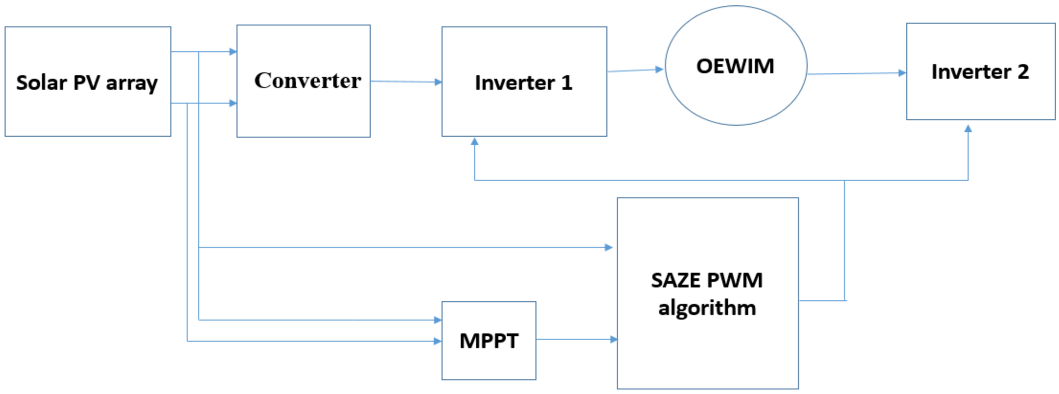

Fig. 1 Block Diagram of Control Algorithms of OEWIM

Nowadays open end winding induction machine received large attention in many applications and has many advantage over conventional induction machine. The proposed system is powered by solar photovoltaic panel and to track the maximum power MPPT algorithm is used. A high voltage gain DC- DC converter is also used to obtain a stable output. The proposed converter is Dickson charge pump voltage multiplier. An OEWIM contains dual inverters on either side of the machine to achieve a three level output voltage and supply is provided from both sides of the inverter. The machine can be used for variable speed applications, grid applications, hybrid vehicles etc.

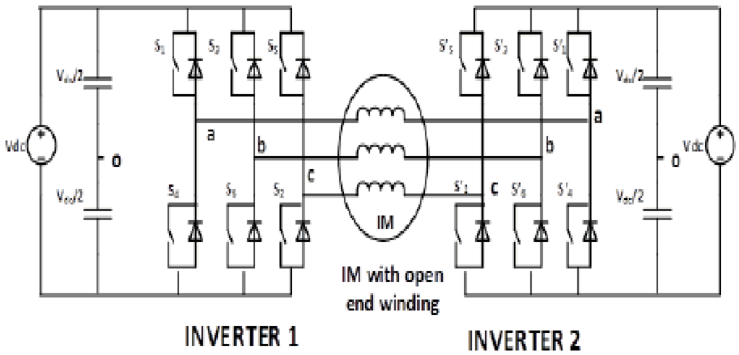

Fig. 2 Open End Winding Induction Motor

Figure 2 shows an induction machine with both ends of stator windings are open. Since both ends of stator windings are open the switches can be rated at half of the machine power rating and it removes the common mode voltage generated due to switching.

III.SIMULATION AND RESULTS

A. *Modeling of Induction Motor*

Modelling of open end winding induction motor is similar to conventional induction motor. Nowadays it is of great importance in both industries and in academics dynamic simulation and modeling of induction motor due to the prevalence of these motors for the validation of design process of drive systems, eliminating design mistakes etc. For simulating the proposed system, a 4 kW induction motor is modelled with the parameters specified in Table1. The dynamic model is obtained by writing differential equations of voltage and torque.

TABLE 1: MOTOR PARAMETERS

Parameter	**Value**	**Parameter**	**Value**
Input voltage	400 V	Stator resistance, R_s	1.405 Ω
Stator current	7.2 A	Stator inductance, L_s	0.0058 H
Rated speed	1430 rpm	Moment of inertia, J	0.0131 kg-m^2
Frequency	50 Hz	Rated torque	26.7 Nm

The stator and rotor voltage equations are as follows.

$$V_{qs} = R_s i_{qs} + \frac{d\varphi_{qs}}{dt} + \omega_e \varphi_{ds} \quad (1)$$

$$V_{ds} = R_s i_{ds} + \frac{d\varphi_{ds}}{dt} + \omega_e \varphi_{qs} \quad (2)$$

$$V_{qr} = R_s i_{qr} + \frac{d\varphi_{qr}}{dt} + \omega_e \varphi_{dr} \quad (3)$$

$$V_{dr} = R_s i_{dr} + \frac{d\varphi_{dr}}{dt} + \omega_e \varphi_{qr} \quad (4)$$

The equation for determining torque and rotor speed of induction motor is given by

$$T_e = \frac{3}{2} * \frac{p}{2} * \frac{1}{w_b} (F_{ds} i_{qs} - F_{qs} i_{ds}) \quad (5)$$

$$T_e = T_l + \frac{2}{p} * J * \frac{dw_r}{dt} \quad (6)$$

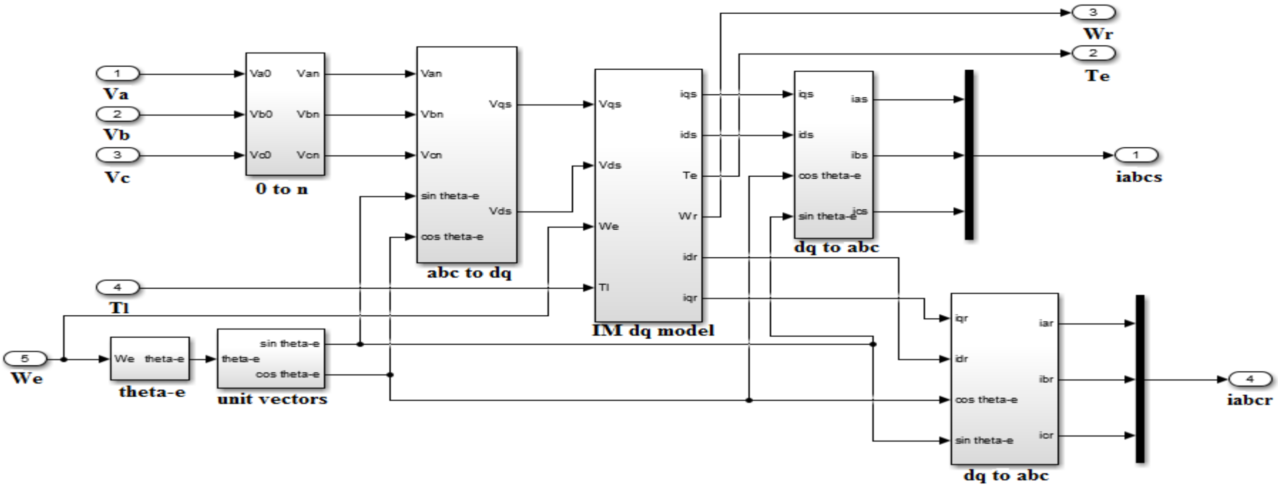

Fig. 3. Modeling of induction motor

Figure 3 shows the modeling of induction motor according to the above voltage and torque equations. The results obtained are as follows. Figure 4 shows the input voltage given to the induction motor with an amplitude of 400 V.

IJIREEICE

ISSN (Online) 2321-2004
ISSN (Print) 2321- 5526

International Journal of Innovative Research in Electrical, Electronics, Instrumentation and Control Engineering

NFTPCOS-18

National Conference on Future Technologies in Power Control and Communication Systems

College of Engineering Perumon, Kollam, Kerala

Vol. 1, Special Issue 2, March 2018

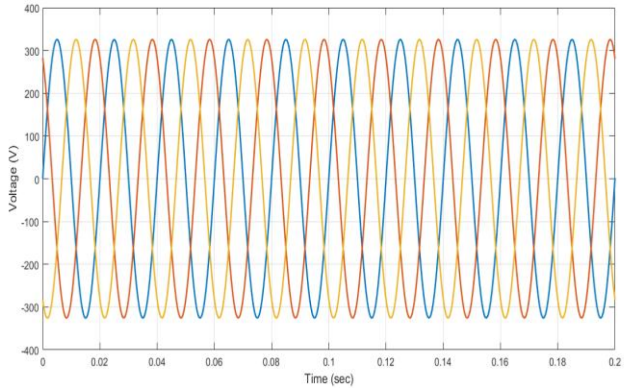

Fig. 4. Input voltage of induction motor

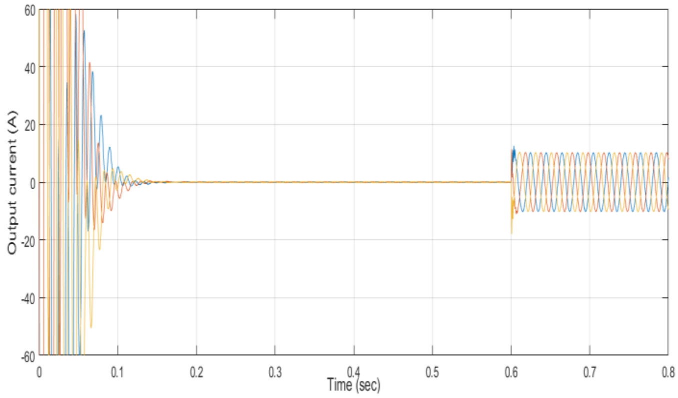

Fig. 5. Output current of induction motor

Figure 5 shows the waveforms of output current, of an induction machine. A step time of 0.6 sec is given to the machine, as a result up to 0.6 sec the graphs shows the no load reading and after 0.6 sec loaded condition is depicted here. The peak value of the current of about 10.2 A obtained.

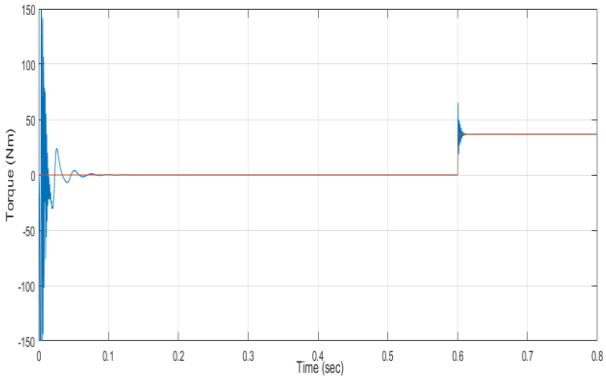

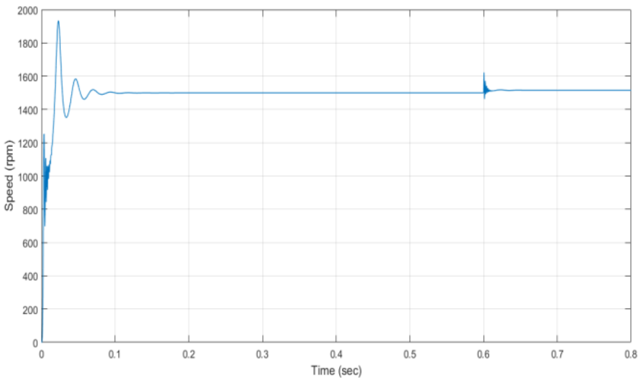

Fig. 6. Torque characteristics of induction motor

Fig. 7. Speed characteristics of induction motor

B. Modeling of PV System

Solar photovoltaic system is used to supply the machine and is modeled for running a 4 kW open end winding induction motor. It is modeled according to the voltage current characteristic equation.

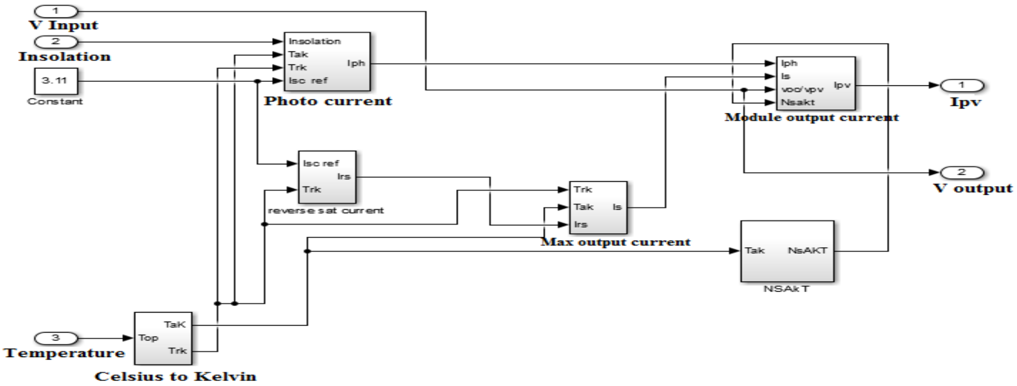

Fig. 8. Modeling of PV system

Figure 8 shows the modeling of photovoltaic system in MATLAB according to the voltage current characteristics equation given below:

$$I = I_{ph} - I_s \left[\exp\left(\frac{q(V+IR_s)}{kT_c A}\right)-1\right] - \frac{V+IR_s}{R_{sh}} \qquad (7)$$

Figure 9 and figure 10 shows the PV and VI characteristics obtained during varying temperatures such as 25˚C, 35˚C, 45˚C, 55˚C.

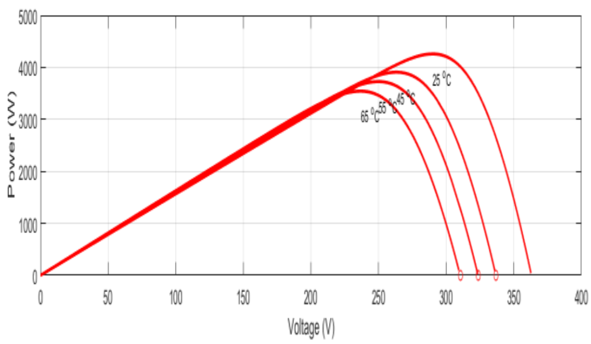

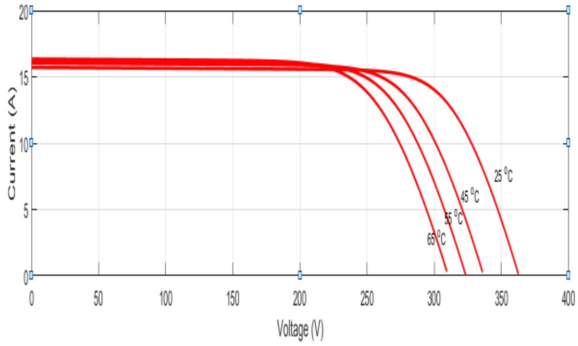

Fig. 9. PV characteristics during varying irradiation

Fig. 10. VI characteristics during varying irradiation

C. Modeling Of MPPT Algorithm

MPPT algorithm can track maximum power and P&O method, one of the most simplest method is proposed here. Figure 11 shows the modeling of MPPT algorithm and the output obtained is used to trigger the converter switches.

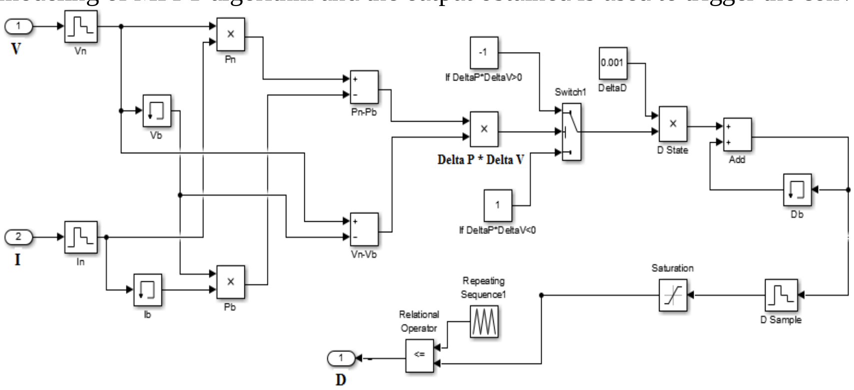

Fig. 11. Modeling of MPPT algorithm

D. Modeling of Converter

IJIREEICE
ISSN (Online) 2321-2004
ISSN (Print) 2321- 5526
International Journal of Innovative Research in Electrical, Electronics, Instrumentation and Control Engineering
NFTPCOS-18
National Conference on Future Technologies in Power Control and Communication Systems
College of Engineering Perumon, Kollam, Kerala
Vol. 1, Special Issue 2, March 2018

To obtain a stable output a converter is also proposed in this circuit. A Dickson charge pump voltage multiplier is used which had a high voltage gain and removes the need of chemical storages such as batteries.

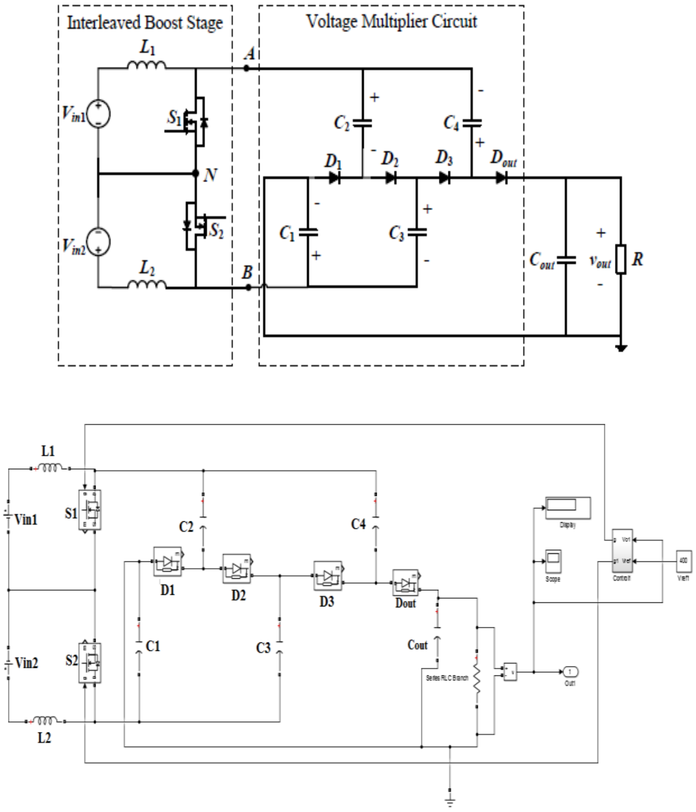

Fig. 12. Dickson charge pump voltage multiplier

Figure 12 shows the circuit of dickon charge pump and MATLAB modeling of converter and this circuit can provide a voltage gain of about 20, such that it can boot 20 V to 400 V which can be shown in Figure 13.

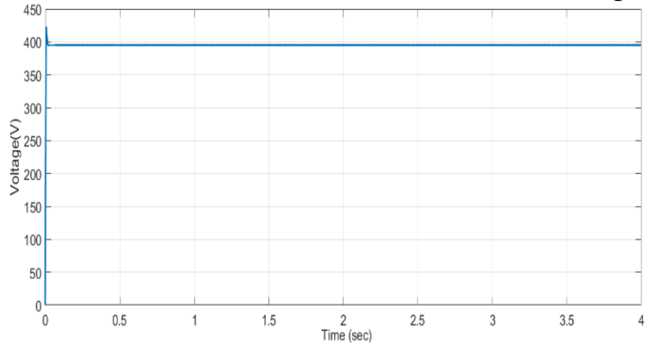

Fig. 13. Output of dickson charge pump voltage multiplier

E. Modeling of Open End Winding Induction Motor and Space Vector Modulation

Modeling of open end winding induction motor is given by subtracting the difference of pole numbers of both the inverters which can be seen in Figure 14. Space vector modulation scheme is used to pulse the switches of the inverter. The modulation scheme will also reduce the effect of common mode voltages generated due to switching of inverters. The following equations are used for converting abc to dq coordinate

$$V_d = \frac{2}{3}\left(V_a \sin\omega t + V_b \sin\left(\omega t - \frac{2\Pi}{3}\right) + V_c \sin\left(\omega t + \frac{2\Pi}{3}\right)\right) \quad (8)$$

$$V_q = \frac{2}{3}\left(V_a \cos\omega t + V_b \cos\left(\omega t - \frac{2\Pi}{3}\right) + V_c \cos\left(\omega t + \frac{2\Pi}{3}\right)\right) \quad (9)$$

$$V_0 = \frac{1}{3}\left(V_a + V_b + V_c\right) \quad (10)$$

ISSN (Online) 2321-2004
ISSN (Print) 2321- 5526

International Journal of Innovative Research in Electrical, Electronics, Instrumentation and Control Engineering

NFTPCOS-18

National Conference on Future Technologies in Power Control and Communication Systems

College of Engineering Perumon, Kollam, Kerala

Vol. 1, Special Issue 2, March 2018

The below equations shows the determination of time duration

$$T_a = \frac{\sqrt{3} * T_Z * V_{ref}}{V_{dc}} \left(\sin\frac{n}{3}\Pi\cos\alpha - \cos\frac{n}{3}\Pi\sin\alpha\right) \quad (11)$$

$$T_b = \frac{\sqrt{3} * T_Z * V_{ref}}{V_{dc}} \left(-\sin\frac{n-1}{3}\Pi\cos\alpha + \cos\frac{n-1}{3}\Pi\sin\alpha\right) \quad (12)$$

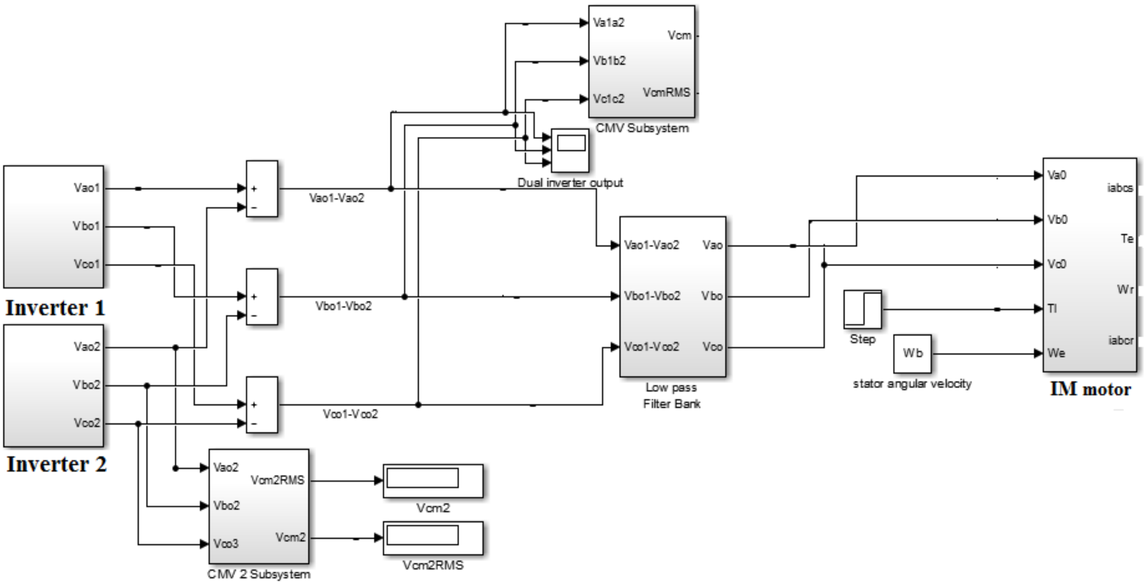

Fig. 14. Modeling of open end winding induction motor

Figure 15 shows the space vector model of the dual inverter. The inverters are pulsed by space vector modulation scheme and is modeled according to the above equations.

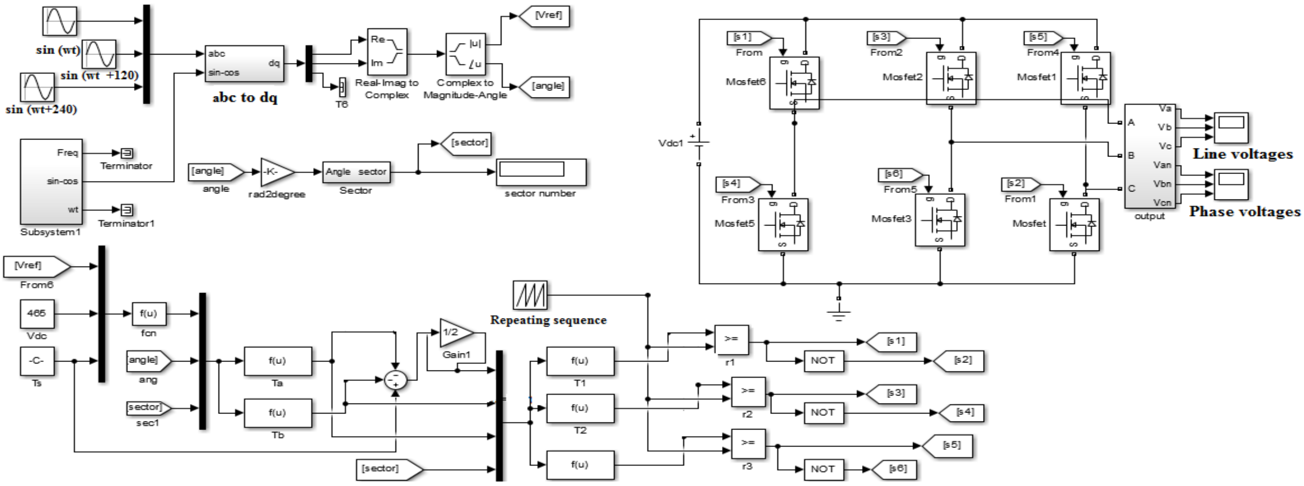

Fig. 15. Modeling inverter and space vector modulation scheme

The modulation scheme has a total of space vector locations of about 64 which can be depicted from the figure 16.

IJIREEICE
ISSN (Online) 2321-2004
ISSN (Print) 2321- 5526
International Journal of Innovative Research in Electrical, Electronics, Instrumentation and Control Engineering
NFTPCOS-18
National Conference on Future Technologies in Power Control and Communication Systems
College of Engineering Perumon, Kollam, Kerala
Vol. 1, Special Issue 2, March 2018

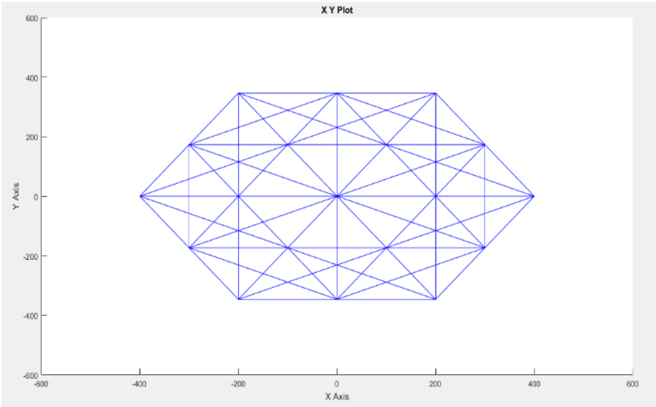

Fig. 16. Space vector of dual inverters

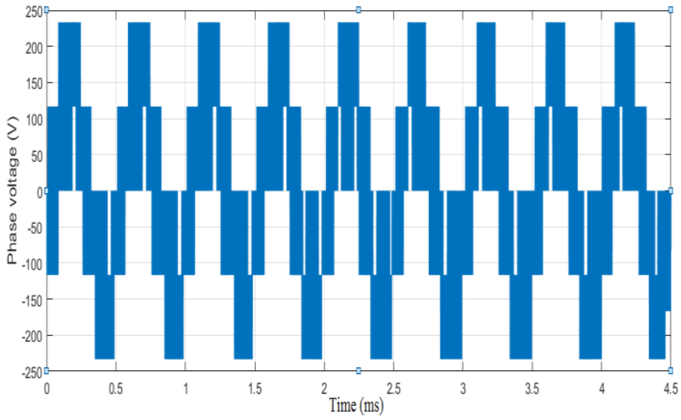

Fig. 17. Dual inverter voltage

Figure 17 shows the dual inverter output voltage obtained by space vector modulation. Dual two level inverters are used to attain the required three level output voltage. The inverter will provide the required voltage required by the open end winding induction motor.

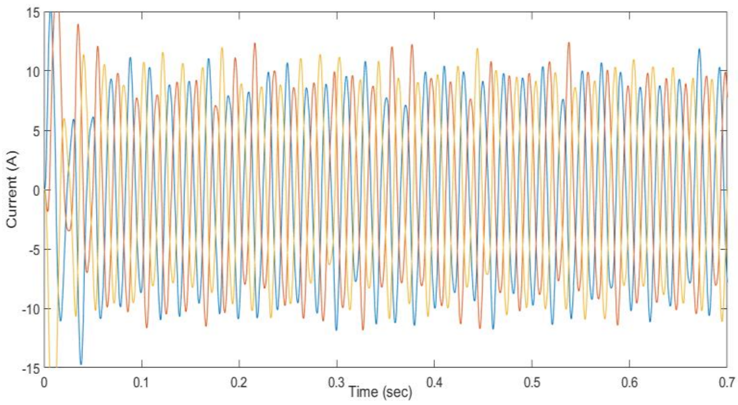

Fig. 18. Output current of open end winding induction motor

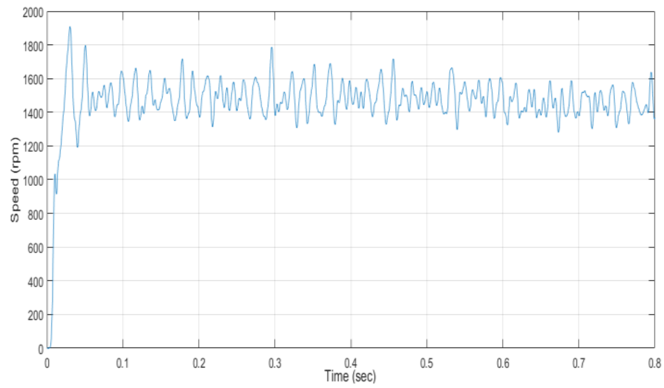

Fig. 19. Speed characteristics

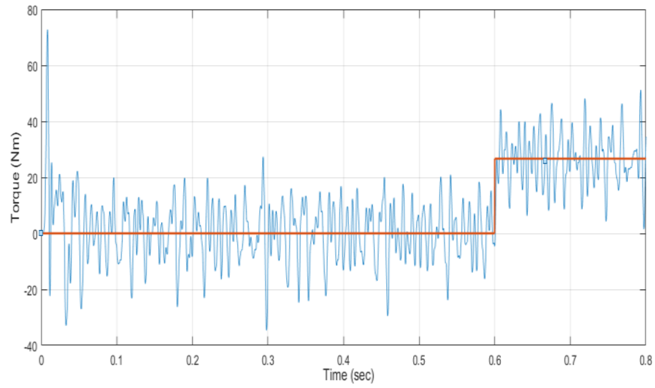

Fig.20. Torque characteristics

Figure 18, 19 and 20 shows the output current, speed and torque of an open end winding induction motor. The dual inverter is modeled and the difference in voltages of inverters is given to induction motor to obtain the modeling of open end winding induction motor. A 0.6 sec a step load is applied and the variation during load can be shown in the figure. The use of open end winding induction motor over conventional machine eliminates the common mode voltages generated.

Common mode voltage is a natural result of pulse width modulation technique and results in disturbance in measuring circuits, motor bearings, EMI problems etc. The common mode voltage of dual inverter drive defined with reference to motor frame is given by:

$$V_{CM} = V_{CM1} - V_{CM2} \quad (13)$$

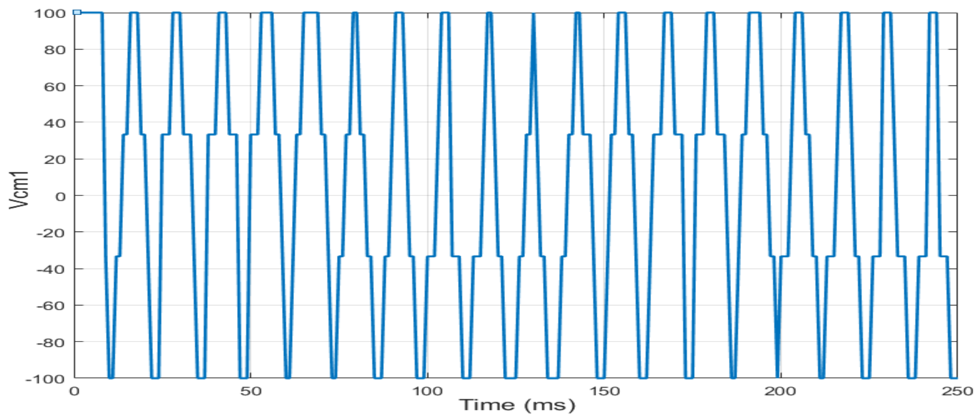

Fig.21. Common mode voltage of inverter 1

Figure 21 shows the common mode voltage of inverter 1 and the same is obtained for inverter 2 and the difference in common mode voltage is obtained equal to zero. Some combinations of space vector locations will give the common mode voltage equivalent to zero which will prevent the machine from damages and proves that the open end winding induction motor is more advantageous than conventional machine.

IV. CONCLUSION

Induction machine with stator end windings are analysed with dual inverters connected to the open end winding induction machine. This offers many advantages over conventional induction machine for pumping applications. Modeling of open end winding induction motor with three level inverter, conventional induction machine, PV system, MPPT are modeled and different output waveforms are analysed. The space vector modulation, which is used to pulse the inverters will avoid the unwanted voltage levels and the occurrence of common mode voltages due to pulse width modulation technique can also be avoided by this technique.

REFERENCES

[1] P. Wheeler, L. Xu, L. Meng Yeong, L. Empringham, C. Klumpner, and J. Clare, “A review of multi-level matrix converter topologies,” in *Proc. 4th IET Conf. Power Electron., Mach. Drives*, 2008, pp. 286–290.
[2] J. Rodriguez, L. Jih-Sheng, and P. Fang Zheng, “Multilevel inverters: A survey of topologies, controls, and applications,” *IEEE Trans. Ind.Electron.*, vol. 49, no. 4, pp. 724–738, Aug. 2002.
[3] J. Rodriguez, S. Bernet, P. K. Steimer, and I. E. Lizama, “A survey on neutral- point-clamped inverters,” *IEEE Trans. Ind. Electron.*, vol. 57, no. 7, pp. 2219–2230, Jul. 2010.
[4] Y. Jiao, S. Lu, and F. C. Lee, “Switching performance optimization of a high power high frequency three-level active neutral point clamped phase leg,” *IEEE Trans. Power Electron.*, vol. 29, no. 7, pp. 3255–3266, Jul. 2014.
[5] P. P. Rajeevan, K. Sivakumar, K. Gopakumar, C. Patel, and H. Abu-Rub, “A nine-level inverter topology for medium-voltage induction motor drive with open-end stator winding,” *IEEE Trans. Ind. Electron.*, vol. 60, no. 9, pp. 3627–3636, Sep. 2013.
[6] V. T. Somasekhar, B. Venugopal Reddy, and K. Sivakumar, “A four-level inversion scheme for a six-*n*-pole open-end winding induction motor drive for an improved DC-link utilization,” *IEEE Trans. Ind. Electron.*, vol. 61, no. 9, pp. 4565–4572, Sep. 2014.
[7] R. Sudharshan Kaarthik, K. Gopakumar, J. Mathew, and T. Undeland, “Medium-voltage drive for induction machine with multilevel dodecagonal voltage space vectors with symmetric triangles,” *IEEE Trans. Ind. Electron.*, vol. 62, no. 1, pp. 79–87, Jan. 2015.
[8] S. Kouro, J. Rodriguez, W. Bin, S. Bernet, and M. Perez, “Powering the future of industry: High-power adjustable speed drive topologies,” *IEEE Ind. Appl. Mag.*, vol. 18, no. 4, pp. 26–39, Jul./Aug. 2012.
[9] F. Betin *et al.*, “Trends in electrical machines control: Samples for classical, sensorless, and fault-tolerant techniques,” *IEEE Ind. Electron. Mag.*, vol. 8, no. 2, pp. 43–55, Jun. 2014.
[10] F. Meinguet, N. Ngac-Ky, P. Sandulescu, X. Kestelyn, and E. Semail, “Fault-tolerant operation of an open-end winding five-phase PMSM drive with inverter faults,” in *Proc. Annu. Conf. IEEE Ind. Electron. Soc.*, 2013, pp. 5191–5196.
[11] N. Ertugrul, W. Soong, G. Dostal, and D. Saxon, “Fault tolerant motor drive system with redundancy for critical applications,” in *Proc. IEEE Power Electron. Spec. Conf.*, 2002, vol. 3, pp. 1457–1462.